

Observation of the Decay $B_s^0 \rightarrow K^0 \bar{K}^0$

B. Pal,⁷ A. J. Schwartz,⁷ A. Abdesselam,⁶⁴ I. Adachi,^{15,12} H. Aihara,⁷¹ D. M. Asner,⁵⁴ T. Aushev,^{42,25} R. Ayad,⁶⁴ T. Aziz,⁶⁵ V. Babu,⁶⁵ I. Badhrees,^{64,30} S. Bahinipati,¹⁷ A. M. Bakich,⁶³ E. Barberio,⁴⁰ P. Behera,¹⁹ V. Bhardwaj,⁶¹ B. Bhuyan,¹⁸ J. Biswal,²⁶ A. Bobrov,^{4,52} A. Bozek,⁴⁹ M. Bračko,^{38,26} T. E. Browder,¹⁴ D. Červenkov,⁵ V. Chekelian,³⁹ A. Chen,⁴⁶ B. G. Cheon,¹³ R. Chistov,²⁵ K. Cho,³¹ V. Chobanova,³⁹ Y. Choi,⁶² D. Cinabro,⁷⁷ J. Dalseno,^{39,66} N. Dash,¹⁷ Z. Doležal,⁵ Z. Drásal,⁵ A. Drutskoy,^{25,41} D. Dutta,⁶⁵ S. Eidelman,^{4,52} H. Farhat,⁷⁷ J. E. Fast,⁵⁴ B. G. Fulsom,⁵⁴ V. Gaur,⁶⁵ A. Garmash,^{4,52} R. Gillard,⁷⁷ Y. M. Goh,¹³ P. Goldenzweig,²⁸ D. Greenwald,⁶⁷ O. Grzymkowska,⁴⁹ J. Haba,^{15,12} T. Hara,^{15,12} K. Hayasaka,⁴⁴ H. Hayashii,⁴⁵ X. H. He,⁵⁵ W.-S. Hou,⁴⁸ K. Inami,⁴³ A. Ishikawa,⁶⁹ Y. Iwasaki,¹⁵ W. W. Jacobs,²⁰ I. Jaegle,¹⁴ H. B. Jeon,³³ D. Joffe,²⁹ K. K. Joo,⁶ T. Julius,⁴⁰ K. H. Kang,³³ E. Kato,⁶⁹ T. Kawasaki,⁵⁰ C. Kiesling,³⁹ D. Y. Kim,⁶⁰ H. J. Kim,³³ K. T. Kim,³² M. J. Kim,³³ S. H. Kim,¹³ K. Kinoshita,⁷ P. Kodyš,⁵ S. Korpar,^{38,26} P. Križan,^{35,26} P. Krokovny,^{4,52} T. Kuhr,³⁶ R. Kumar,⁵⁷ T. Kumita,⁷³ A. Kuzmin,^{4,52} Y.-J. Kwon,⁷⁹ I. S. Lee,¹³ C. H. Li,⁴⁰ H. Li,²⁰ L. Li,⁵⁸ L. Li Gioi,³⁹ J. Libby,¹⁹ D. Liventsev,^{76,15} P. Lukin,^{4,52} T. Luo,⁵⁶ M. Masuda,⁷⁰ D. Matvienko,^{4,52} K. Miyabayashi,⁴⁵ H. Miyata,⁵⁰ R. Mizuk,^{25,41} G. B. Mohanty,⁶⁵ S. Mohanty,^{65,75} A. Moll,^{39,66} H. K. Moon,³² T. Mori,⁴³ R. Mussa,²⁴ E. Nakano,⁵³ M. Nakao,^{15,12} T. Nanut,²⁶ Z. Natkaniec,⁴⁹ M. Nayak,¹⁹ N. K. Nisar,^{65,1} S. Nishida,^{15,12} S. Ogawa,⁶⁸ S. Okuno,²⁷ P. Pakhlov,^{25,41} G. Pakhlova,^{42,25} C. W. Park,⁶² H. Park,³³ S. Paul,⁶⁷ T. K. Pedlar,³⁷ L. Pesántez,³ R. Pestotnik,²⁶ M. Petrič,²⁶ L. E. Piilonen,⁷⁶ C. Pulvermacher,²⁸ J. Rauch,⁶⁷ E. RIBEŽIČ,²⁶ M. Ritter,³⁶ A. Rostomyan,⁸ S. Ryu,⁵⁹ H. Sahoo,¹⁴ Y. Sakai,^{15,12} S. Sandilya,⁶⁵ T. Sanuki,⁶⁹ Y. Sato,⁴³ V. Savinov,⁵⁶ T. Schlüter,³⁶ O. Schneider,³⁴ G. Schnell,^{2,16} C. Schwanda,²² Y. Seino,⁵⁰ K. Senyo,⁷⁸ O. Seon,⁴³ I. S. Seong,¹⁴ V. Shebalin,^{4,52} T.-A. Shibata,⁷² J.-G. Shiu,⁴⁸ B. Shwartz,^{4,52} F. Simon,^{39,66} Y.-S. Sohn,⁷⁹ A. Sokolov,²³ E. Solovieva,²⁵ S. Stanič,⁵¹ M. Starič,²⁶ J. Stypula,⁴⁹ M. Sumihama,¹¹ T. Sumiyoshi,⁷³ U. Tamponi,^{24,74} Y. Teramoto,⁵³ K. Trabelsi,^{15,12} M. Uchida,⁷² S. Uehara,^{15,12} T. Uglov,^{25,42} S. Uno,^{15,12} P. Urquijo,⁴⁰ Y. Usov,^{4,52} C. Van Hulse,² P. Vanhoefer,³⁹ G. Varner,¹⁴ A. Vinokurova,^{4,52} A. Vossen,²⁰ M. N. Wagner,¹⁰ C. H. Wang,⁴⁷ M.-Z. Wang,⁴⁸ X. L. Wang,⁷⁶ M. Watanabe,⁵⁰ Y. Watanabe,²⁷ K. M. Williams,⁷⁶ E. Won,³² J. Yamaoka,⁵⁴ J. Yelton,⁹ C. Z. Yuan,²¹ Y. Yusa,⁵⁰ Z. P. Zhang,⁵⁸ V. Zhilich,^{4,52} V. Zhulanov,^{4,52} and A. Zupanc^{35,26}

(Belle Collaboration)

¹Aligarh Muslim University, Aligarh 202002

²University of the Basque Country UPV/EHU, 48080 Bilbao

³University of Bonn, 53115 Bonn

⁴Budker Institute of Nuclear Physics SB RAS, Novosibirsk 630090

⁵Faculty of Mathematics and Physics, Charles University, 12116 Prague

⁶Chonnam National University, Kwangju 660-701

⁷University of Cincinnati, Cincinnati, Ohio 45221

⁸Deutsches Elektronen-Synchrotron, 22607 Hamburg

⁹University of Florida, Gainesville, Florida 32611

¹⁰Justus-Liebig-Universität Gießen, 35392 Gießen

¹¹Gifu University, Gifu 501-1193

¹²SOKENDAI (The Graduate University for Advanced Studies), Hayama 240-0193

¹³Hanyang University, Seoul 133-791

¹⁴University of Hawaii, Honolulu, Hawaii 96822

¹⁵High Energy Accelerator Research Organization (KEK), Tsukuba 305-0801

¹⁶IKERBASQUE, Basque Foundation for Science, 48013 Bilbao

¹⁷Indian Institute of Technology Bhubaneswar, Satya Nagar 751007

¹⁸Indian Institute of Technology Guwahati, Assam 781039

¹⁹Indian Institute of Technology Madras, Chennai 600036

²⁰Indiana University, Bloomington, Indiana 47408

²¹Institute of High Energy Physics, Chinese Academy of Sciences, Beijing 100049

²²Institute of High Energy Physics, Vienna 1050

²³Institute for High Energy Physics, Protvino 142281

²⁴INFN-Sezione di Torino, 10125 Torino

²⁵Institute for Theoretical and Experimental Physics, Moscow 117218

²⁶J. Stefan Institute, 1000 Ljubljana

²⁷Kanagawa University, Yokohama 221-8686

- ²⁸*Institut für Experimentelle Kernphysik, Karlsruher Institut für Technologie, 76131 Karlsruhe*
²⁹*Kennesaw State University, Kennesaw, Georgia 30144*
³⁰*King Abdulaziz City for Science and Technology, Riyadh 11442*
³¹*Korea Institute of Science and Technology Information, Daejeon 305-806*
³²*Korea University, Seoul 136-713*
³³*Kyungpook National University, Daegu 702-701*
³⁴*École Polytechnique Fédérale de Lausanne (EPFL), Lausanne 1015*
³⁵*Faculty of Mathematics and Physics, University of Ljubljana, 1000 Ljubljana*
³⁶*Ludwig Maximilians University, 80539 Munich*
³⁷*Luther College, Decorah, Iowa 52101*
³⁸*University of Maribor, 2000 Maribor*
³⁹*Max-Planck-Institut für Physik, 80805 München*
⁴⁰*School of Physics, University of Melbourne, Victoria 3010*
⁴¹*Moscow Physical Engineering Institute, Moscow 115409*
⁴²*Moscow Institute of Physics and Technology, Moscow Region 141700*
⁴³*Graduate School of Science, Nagoya University, Nagoya 464-8602*
⁴⁴*Kobayashi-Maskawa Institute, Nagoya University, Nagoya 464-8602*
⁴⁵*Nara Women's University, Nara 630-8506*
⁴⁶*National Central University, Chung-li 32054*
⁴⁷*National United University, Miao Li 36003*
⁴⁸*Department of Physics, National Taiwan University, Taipei 10617*
⁴⁹*H. Niewodniczanski Institute of Nuclear Physics, Krakow 31-342*
⁵⁰*Niigata University, Niigata 950-2181*
⁵¹*University of Nova Gorica, 5000 Nova Gorica*
⁵²*Novosibirsk State University, Novosibirsk 630090*
⁵³*Osaka City University, Osaka 558-8585*
⁵⁴*Pacific Northwest National Laboratory, Richland, Washington 99352*
⁵⁵*Peking University, Beijing 100871*
⁵⁶*University of Pittsburgh, Pittsburgh, Pennsylvania 15260*
⁵⁷*Punjab Agricultural University, Ludhiana 141004*
⁵⁸*University of Science and Technology of China, Hefei 230026*
⁵⁹*Seoul National University, Seoul 151-742*
⁶⁰*Soongsil University, Seoul 156-743*
⁶¹*University of South Carolina, Columbia, South Carolina 29208*
⁶²*Sungkyunkwan University, Suwon 440-746*
⁶³*School of Physics, University of Sydney, New South Wales 2006*
⁶⁴*Department of Physics, Faculty of Science, University of Tabuk, Tabuk 71451*
⁶⁵*Tata Institute of Fundamental Research, Mumbai 400005*
⁶⁶*Excellence Cluster Universe, Technische Universität München, 85748 Garching*
⁶⁷*Department of Physics, Technische Universität München, 85748 Garching*
⁶⁸*Toho University, Funabashi 274-8510*
⁶⁹*Department of Physics, Tohoku University, Sendai 980-8578*
⁷⁰*Earthquake Research Institute, University of Tokyo, Tokyo 113-0032*
⁷¹*Department of Physics, University of Tokyo, Tokyo 113-0033*
⁷²*Tokyo Institute of Technology, Tokyo 152-8550*
⁷³*Tokyo Metropolitan University, Tokyo 192-0397*
⁷⁴*University of Torino, 10124 Torino*
⁷⁵*Utkal University, Bhubaneswar 751004*
⁷⁶*CNP, Virginia Polytechnic Institute and State University, Blacksburg, Virginia 24061*
⁷⁷*Wayne State University, Detroit, Michigan 48202*
⁷⁸*Yamagata University, Yamagata 990-8560*
⁷⁹*Yonsei University, Seoul 120-749*

(Received 7 December 2015; published 19 April 2016)

We measure the decay $B_s^0 \rightarrow K^0 \bar{K}^0$ using data collected at the $\Upsilon(5S)$ resonance with the Belle detector at the KEKB e^+e^- collider. The data sample used corresponds to an integrated luminosity of 121.4 fb^{-1} . We measure a branching fraction $\mathcal{B}(B_s^0 \rightarrow K^0 \bar{K}^0) = [19.6_{-5.1}^{+5.8}(\text{stat}) \pm 1.0(\text{syst}) \pm 2.0(N_{B_s^0 \bar{B}_s^0})] \times 10^{-6}$ with a significance of 5.1 standard deviations. This measurement constitutes the first observation of this decay.

DOI: 10.1103/PhysRevLett.116.161801

The two-body decays $B_s^0 \rightarrow h^+ h'^-$, where $h^{(\prime)}$ is either a pion or kaon, have now all been observed [1]. In contrast, the neutral-daughter decays $B_s^0 \rightarrow h^0 h'^0$ have yet to be observed. The decay $B_s^0 \rightarrow K^0 \bar{K}^0$ [2] is of particular interest because the branching fraction is predicted to be relatively large. In the standard model (SM), the decay proceeds mainly via a $b \rightarrow s$ loop (or “penguin”) transition as shown in Fig. 1, and the branching fraction is predicted to be in the range $(16\text{--}27) \times 10^{-6}$ [3]. The presence of non-SM particles or couplings could enhance this value [4]. It has been pointed out that CP asymmetries in $B_s^0 \rightarrow K^0 \bar{K}^0$ decays are promising observables in which to search for new physics [5].

The current upper limit on the branching fraction, $\mathcal{B}(B_s^0 \rightarrow K^0 \bar{K}^0) < 6.6 \times 10^{-5}$ at 90% confidence level, was set by the Belle Collaboration using 23.6 fb^{-1} of data recorded at the $\Upsilon(5S)$ resonance [6]. Here, we update this result using the full data set of 121.4 fb^{-1} recorded at the $\Upsilon(5S)$. The analysis presented here uses improved tracking, K^0 reconstruction, and continuum suppression algorithms. The data set corresponds to $(6.53 \pm 0.66) \times 10^6$ $B_s^0 \bar{B}_s^0$ pairs [7] produced in three $\Upsilon(5S)$ decay channels: $B_s^0 \bar{B}_s^0$, $B_s^{*0} \bar{B}_s^0$ or $B_s^0 \bar{B}_s^{*0}$, and $B_s^{*0} \bar{B}_s^{*0}$. The latter two channels dominate, with production fractions of $f_{B_s^0 \bar{B}_s^0} = (7.3 \pm 1.4)\%$ and $f_{B_s^{*0} \bar{B}_s^{*0}} = (87.0 \pm 1.7)\%$ [8].

The Belle detector is a large-solid-angle magnetic spectrometer consisting of a silicon vertex detector (SVD), a 50-layer central drift chamber (CDC), an array of aerogel threshold Cherenkov counters, a barrel-like arrangement of time-of-flight scintillation counters, and an electromagnetic calorimeter comprising CsI(Tl) crystals. These detector components are located inside a superconducting solenoid coil that provides a 1.5 T magnetic field. An iron flux return located outside the coil is instrumented to detect K_L^0 mesons and to identify muons. The detector is described in detail elsewhere [9,10]. The origin of the coordinate system is defined as the position of the nominal interaction point (IP). The $+z$ axis is aligned with the direction opposite the e^+ beam and is parallel to the direction of the magnetic field within the solenoid. The $+x$ axis is horizontal and points towards the outside of the storage ring; the $+y$ axis points vertically upward.

Candidate K^0 mesons are reconstructed via the decay $K_S^0 \rightarrow \pi^+ \pi^-$ using a neural network (NN) technique [11]. The NN uses the following information: the K_S^0 momentum in the laboratory frame; the distance along z between the

two track helices at their closest approach; the flight length in the x - y plane; the angle between the K_S^0 momentum, and the vector joining the K_S^0 decay vertex to the IP; the angle between the pion momentum and the laboratory-frame direction in the K_S^0 rest frame; the distance-of-closest-approach in the x - y plane between the IP and the two pion helices; and the pion hit information in the SVD and CDC. The selection efficiency is 87% over the momentum range of interest. We also require that the $\pi^+ \pi^-$ invariant mass be within 12 MeV/ c^2 (about 3.5σ in resolution) of the nominal K_S^0 mass [1].

To identify $B_s^0 \rightarrow K_S^0 K_S^0$ candidates, we define two variables: the beam-energy-constrained mass $M_{bc} = \sqrt{E_{\text{beam}}^2 - |\vec{p}_B|^2 c^2}/c^2$; and the energy difference $\Delta E = E_B - E_{\text{beam}}$, where E_{beam} is the beam energy and E_B and \vec{p}_B are the energy and momentum, respectively, of the B_s^0 candidate. These quantities are evaluated in the $e^+ e^-$ center-of-mass frame. We require that events satisfy $M_{bc} > 5.34 \text{ GeV}/c^2$ and $-0.20 \text{ GeV} < \Delta E < 0.10 \text{ GeV}$.

To suppress the background arising from continuum $e^+ e^- \rightarrow q\bar{q}$ ($q = u, d, s, c$) production, we use a second NN [11] that distinguishes jetlike continuum events from more spherical $B_s^{(*)0} \bar{B}_s^{(*)0}$ events. This NN uses the following input variables, which characterize the event topology: the cosine of the angle between the thrust axis [12] of the B_s^0 candidate and the thrust axis of the rest of the event; the cosine of the angle between the B_s^0 thrust axis and the $+z$ axis; a set of 16 modified Fox-Wolfram moments [13]; and the ratio of the second to zeroth (unmodified) Fox-Wolfram moments. All quantities are evaluated in the center-of-mass frame. The NN is trained using Monte Carlo (MC) simulated signal events and $q\bar{q}$ background events. The MC samples are obtained using EVTGEN [14] for event generation and GEANT3[15] for modeling the detector response. The NN has a single output variable (C_{NN}) that ranges from -1 for backgroundlike events to $+1$ for signal-like events. We require $C_{\text{NN}} > -0.1$, which rejects approximately 85% of $q\bar{q}$ background while retaining 83% of signal decays. We subsequently translate C_{NN} to a new variable

$$C'_{\text{NN}} = \ln \left(\frac{C_{\text{NN}} - C_{\text{NN}}^{\min}}{C_{\text{NN}}^{\max} - C_{\text{NN}}} \right), \quad (1)$$

where $C_{\text{NN}}^{\min} = -0.1$ and C_{NN}^{\max} is the maximum value of C_{NN} obtained from a large sample of signal MC decays. The distribution of C'_{NN} is well modeled by a Gaussian function.

After applying all selection criteria, approximately 1.0% of the events have multiple B_s^0 candidates. For these events, we retain the candidate having the smallest value of χ^2 obtained from the deviations of the reconstructed K_S^0 masses from their nominal values [1]. According to MC simulation, this criterion selects the correct B_s^0 candidate $> 99\%$ of the time.

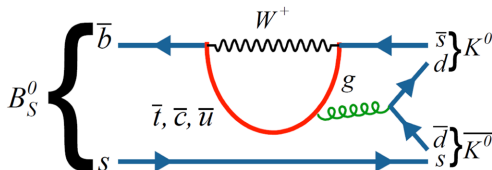


FIG. 1. Loop diagram for $B_s^0 \rightarrow K^0 \bar{K}^0$ decays.

We measure the signal yield by performing an unbinned extended maximum likelihood fit to the variables M_{bc} , ΔE , and C'_{NN} . The likelihood function is defined as

$$\mathcal{L} = e^{-\sum_j Y_j} \prod_i \left(\sum_j Y_j \mathcal{P}_j(M_{bc}^i, \Delta E^i, C'_{NN}{}^i) \right), \quad (2)$$

where Y_j is the yield of component j ; $\mathcal{P}_j(M_{bc}^i, \Delta E^i, C'_{NN}{}^i)$ is the probability density function (PDF) of component j for event i ; j runs over the two event categories (signal and $q\bar{q}$ background); and i runs over all events in the sample (N). Backgrounds arising from other B_s^0 and non- B_s^0 decays were studied using MC simulation and found to be negligible. As correlations among the variables M_{bc} , ΔE , and C'_{NN} are found to be small, the three-dimensional PDFs $\mathcal{P}_j(M_{bc}^i, \Delta E^i, C'_{NN}{}^i)$ are factorized into the product of separate one-dimensional PDFs.

The signal PDF is defined as

$$\mathcal{P}_{\text{sig}} = f_{B_s^{*0}\bar{B}_s^0} \mathcal{P}_{B_s^{*0}\bar{B}_s^0} + f_{B_s^0\bar{B}_s^0} \mathcal{P}_{B_s^0\bar{B}_s^0} + (1 - f_{B_s^{*0}\bar{B}_s^0} - f_{B_s^0\bar{B}_s^0}) \mathcal{P}_{B_s^0\bar{B}_s^0}, \quad (3)$$

where $\mathcal{P}_{B_s^{*0}\bar{B}_s^0}$, $\mathcal{P}_{B_s^0\bar{B}_s^0}$, and $\mathcal{P}_{B_s^0\bar{B}_s^0}$ are the PDFs for signal arising from $\Upsilon(5S) \rightarrow B_s^{*0}\bar{B}_s^0$, $(B_s^{*0}\bar{B}_s^0 + B_s^0\bar{B}_s^0)$, and $B_s^0\bar{B}_s^0$ decays. The M_{bc} and C'_{NN} PDFs are modeled with Gaussian functions, and the ΔE PDFs are each modeled with a sum of two Gaussian functions having a common mean. All parameters of the signal PDF are fixed to the corresponding MC values. The peak positions for M_{bc} and ΔE are adjusted according to small data-MC differences observed in a control sample of $B_s^0 \rightarrow D_s^- \pi^+$ decays [8]. As this control sample has only modest statistics, the resolutions for M_{bc} , ΔE , and C'_{NN} , and the peak position for C'_{NN} , are adjusted for data-MC differences using a high statistics sample of $B^0 \rightarrow D^-(\rightarrow K^+ \pi^- \pi^-) \pi^+$ decays. For $q\bar{q}$ background, the M_{bc} , ΔE , and C'_{NN} PDFs are modeled with an ARGUS function [16], a first-order Chebyshev

polynomial, and a Gaussian function, respectively. All parameters of the $q\bar{q}$ background PDFs except for the end point of the ARGUS function are floated in the fit.

The results of the fit are $29.0_{-7.6}^{+8.5}$ signal events and $1095.0_{-33.4}^{+33.9}$ continuum background events. Projections of the fit are shown in Fig. 2. The branching fraction is calculated via

$$\mathcal{B}(B_s^0 \rightarrow K^0 \bar{K}^0) = \frac{Y_s}{2N_{B_s^0\bar{B}_s^0} \mathcal{B}_{K^0}^2 \mathcal{B}_{K^0}^2 \varepsilon}, \quad (4)$$

where Y_s is the fitted signal yield; $N_{B_s^0\bar{B}_s^0} = (6.53 \pm 0.66) \times 10^6$ is the number of $B_s^0\bar{B}_s^0$ events; $\mathcal{B}_{K^0} = (69.20 \pm 0.05)\%$ is the branching fraction for $K_S^0 \rightarrow \pi^+ \pi^-$ [1]; and $\varepsilon = (46.3 \pm 0.1)\%$ is the signal efficiency as determined from MC simulation. The efficiency is corrected by a factor 1.01 ± 0.02 for each reconstructed K_S^0 , to account for a small difference in K_S^0 reconstruction efficiency between data and simulation. This correction is estimated from a high statistics sample of $D^0 \rightarrow K_S^0 \pi^0$ decays. The factor 0.50 accounts for the 50% probability for $K^0 \bar{K}^0 \rightarrow K_S^0 K_S^0$ (since $K^0 \bar{K}^0$ is CP even). Inserting these values gives $\mathcal{B}(B_s^0 \rightarrow K^0 \bar{K}^0) = (19.6_{-5.1}^{+5.8}) \times 10^{-6}$, where the error is statistical.

The systematic uncertainty on $\mathcal{B}(B_s^0 \rightarrow K^0 \bar{K}^0)$ arises from several sources, as listed in Table I. The uncertainties due to the fixed parameters in the PDF shape are estimated by varying the parameters individually according to their statistical uncertainties. For each variation the branching fraction is recalculated, and the difference with the nominal branching fraction is taken as the systematic uncertainty associated with that parameter. We add together all uncertainties in quadrature to obtain the overall uncertainty due to fixed parameters. The uncertainties due to errors in the calibration factors and the fractions $f_{B_s^{(*)}\bar{B}_s^{(*)}}$ are evaluated in a similar manner. To test the stability of our fitting procedure, we generate

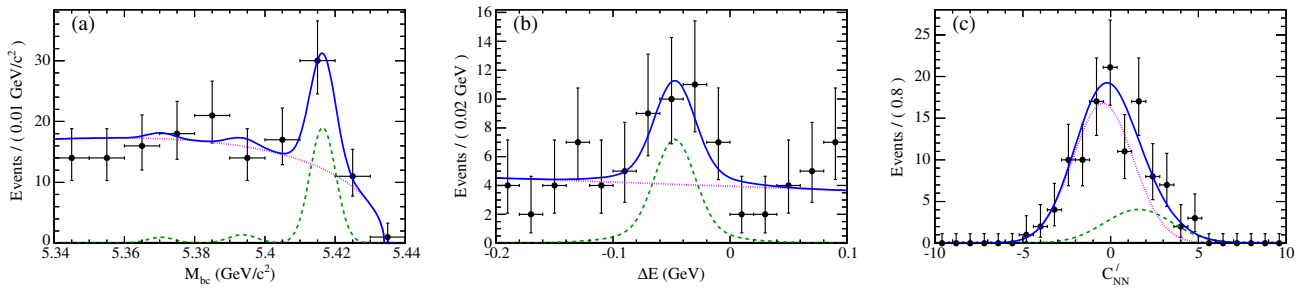


FIG. 2. Projections of the 3D fit to the real data: (a) M_{bc} in $-0.11 \text{ GeV} < \Delta E < 0.02 \text{ GeV}$ and $C'_{NN} > 0.5$; (b) ΔE in $5.405 \text{ GeV}/c^2 < M_{bc} < 5.427 \text{ GeV}/c^2$ and $C'_{NN} > 0.5$; and (c) C'_{NN} in $5.405 \text{ GeV}/c^2 < M_{bc} < 5.427 \text{ GeV}/c^2$ and $-0.11 \text{ GeV} < \Delta E < 0.02 \text{ GeV}$. The points with error bars are data, the (green) dashed curves show the signal, (magenta) dotted curves show the continuum background, and (blue) solid curves show the total. The $\chi^2/(\text{number of bins})$ values of these fit projections are 0.30, 0.43, and 0.26, respectively, which indicate that the fit gives a good description of the data. The three peaks in M_{bc} arise from $\Upsilon(5S) \rightarrow B_s^0\bar{B}_s^0$, $(B_s^{*0}\bar{B}_s^0 + B_s^0\bar{B}_s^0)$, and $B_s^{*0}\bar{B}_s^0$ decays.

TABLE I. Systematic uncertainties on $\mathcal{B}(B_s^0 \rightarrow K^0 \bar{K}^0)$. Those listed in the upper section are associated with fitting for the signal yields and are included in the signal significance.

Source	Uncertainty (%)
PDF parametrization	0.2
Calibration factor	+0.9 -0.8
$f_{B_s^{(*)}\bar{B}_s^{(*)}}$	+1.2 -1.1
Fit bias	+0.0 -2.6
$K_S^0 \rightarrow \pi^+\pi^-$ reconstruction	4.0
C_{NN} selection	0.9
MC sample size	0.2
$\mathcal{B}(K_S^0 \rightarrow \pi^+\pi^-)$	0.1
Total (without $N_{B_s^0\bar{B}_s^0}$)	+4.4 -5.1
$N_{B_s^0\bar{B}_s^0}$	10.1

and fit a large ensemble of MC pseudoexperiments. By comparing the mean of the fitted yields with the input value, a bias of -2.6% is found. We attribute this bias to our neglecting small correlations among the fitted observables. An 0.9% systematic uncertainty is assigned due to the C_{NN} selection; this is obtained by comparing the selection efficiencies in MC simulation and data for the $B^0 \rightarrow D^-(\rightarrow K^+\pi^-\pi^-)\pi^+$ control sample. We assign a 2.0% systematic uncertainty for each reconstructed $K_S^0 \rightarrow \pi^+\pi^-$; this is determined using the $D^0 \rightarrow K_S^0\pi^0$ sample. The uncertainty on ϵ due to the MC sample size is 0.2% . The total of the above systematic uncertainties is calculated as their sum in quadrature. In addition, there is a 10.1% uncertainty due to the number of $B_s^0\bar{B}_s^0$ pairs. As this large uncertainty does not arise from our analysis, we quote it separately.

The signal significance is calculated as $\sqrt{-2\ln(\mathcal{L}_0/\mathcal{L}_{\text{max}})}$, where \mathcal{L}_0 is the likelihood value when the signal yield is fixed to zero, and \mathcal{L}_{max} is the likelihood value of the nominal fit. We include systematic uncertainties in the significance by convolving the likelihood function with a Gaussian function whose width is equal to that part of the systematic uncertainty that affects the signal yield. We obtain a signal significance of 5.1 standard deviations; thus, our measurement constitutes the first observation of this decay.

Figure 3 shows the background-subtracted $sPlot$ [17] distributions of $M(\pi^+\pi^-)$, where the K_S^0 selection is removed for the $\pi^+\pi^-$ pair being plotted. No $B_s^0 \rightarrow K_S^0\pi^+\pi^-$ contribution is observed. We check this quantitatively by performing our signal fit for events in the mass sidebands of each K_S^0 [$M(\pi^+\pi^-) \in (0.460, 0.485) \text{ GeV}/c^2$ and $M(\pi^+\pi^-) \in (0.510, 0.530) \text{ GeV}/c^2$]. The extracted signal yields, $-0.7^{+2.9}_{-2.1}$ and $1.6^{+2.2}_{-1.2}$ for the higher momentum K_S^0 and lower momentum K_S^0 , respectively, are consistent with zero. We calculate the expected number of

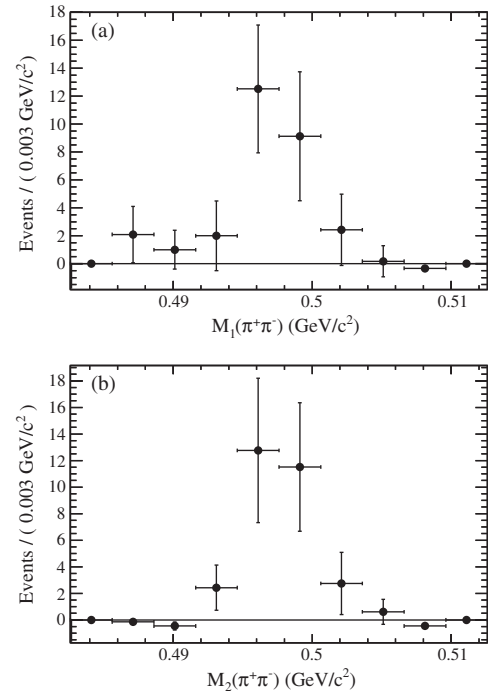


FIG. 3. Background subtracted $sPlot$ distributions of $M(\pi^+\pi^-)$ for the (a) higher momentum and (b) lower momentum K_S^0 candidates.

$B_s^0 \rightarrow K_S^0\pi^+\pi^-$ events in our signal sample using MC simulation and the measured branching fraction, $\mathcal{B}(B_s^0 \rightarrow K^0\pi^+\pi^-) = 15.0 \times 10^{-6}$ [18]; the result is 0.001.

In summary, we report the first observation of the decay $B_s^0 \rightarrow K^0\bar{K}^0$. The branching fraction is measured to be

$$\mathcal{B}(B_s^0 \rightarrow K^0\bar{K}^0) = (19.6^{+5.8}_{-5.1} \pm 1.0 \pm 2.0) \times 10^{-6},$$

where the first uncertainty is statistical, the second is systematic, and the third reflects the uncertainty due to the total number of $B_s^0\bar{B}_s^0$ pairs. This value is in good agreement with the SM predictions [3], and it implies that the Belle II experiment [19] will reconstruct over 1000 of these decays. Such a sample would allow for a much higher sensitivity search for new physics in this $b \rightarrow s$ penguin-dominated decay.

We thank the KEKB group for the excellent operation of the accelerator; the KEK cryogenics group for the efficient operation of the solenoid; and the KEK computer group, the National Institute of Informatics, and the PNNL/EMSL computing group for valuable computing and SINET4 network support. We acknowledge support from the Ministry of Education, Culture, Sports, Science, and Technology (MEXT) of Japan, the Japan Society for the Promotion of Science (JSPS), and the Tau-Lepton Physics Research Center of Nagoya University; the Australian Research Council; Austrian Science Fund under Grants No. P 22742-N16 and No. P 26794-N20; the National Natural Science

Foundation of China under Contracts No. 10575109, No. 10775142, No. 10875115, No. 11175187, and No. 11475187; the Chinese Academy of Science Center for Excellence in Particle Physics; the Ministry of Education, Youth and Sports of the Czech Republic under Contract No. LG14034; the Carl Zeiss Foundation, the Deutsche Forschungsgemeinschaft and the VolkswagenStiftung; the Department of Science and Technology of India; the Istituto Nazionale di Fisica Nucleare of Italy; the WCU program of the Ministry of Education, National Research Foundation (NRF) of Korea Grants No. 2011-0029457, No. 2012-0008143, No. 2012R1A1A2008330, No. 2013R1A1A3007772, No. 2014R1A2A2A01005286, No. 2014R1A2A2A01002734, No. 2015R1A2A2A01003280, No. 2015H1A2A1033649; the Basic Research Lab program under NRF Grant No. KRF-2011-0020333, Center for Korean J-PARC Users, No. NRF-2013K1A3A7A06056592; the Brain Korea 21-Plus program and Radiation Science Research Institute; the Polish Ministry of Science and Higher Education and the National Science Center; the Ministry of Education and Science of the Russian Federation and the Russian Foundation for Basic Research; the Slovenian Research Agency; the Basque Foundation for Science (IKERBASQUE) and the Euskal Herriko Unibertsitatea (UPV/EHU) under program UFI 11/55 (Spain); the Swiss National Science Foundation; the National Science Council and the Ministry of Education of Taiwan; and the U.S. Department of Energy and the National Science Foundation. This work is supported by a Grant-in-Aid from MEXT for Science Research in a Priority Area (“New Development of Flavor Physics”) and from JSPS for Creative Scientific Research (“Evolution of Tau-lepton Physics”).

-
- [1] K. A. Olive *et al.* (Particle Data Group), Review of particle physics, *Chin. Phys. C* **38**, 090001 (2014).
- [2] Unless stated otherwise, charge-conjugate modes are implicitly included.
- [3] C. H. Chen, Analysis of $B_s \rightarrow KK$ decays in the PQCD, *Phys. Lett. B* **520**, 33 (2001); A. R. Williamson and J. Zupan, Two body B decays with isosinglet final states in SCET, *Phys. Rev. D* **74**, 014003 (2006); A. Ali, G. Kramer, Y. Li, C. D. Lu, Y. L. Shen, W. Wang, and Y. M. Wang, Charmless non-leptonic B_s decays to PP , PV , and VV final states in the pQCD approach, *Phys. Rev. D* **76**, 074018 (2007); C. K. Chua, Rescattering effects in charmless $\bar{B}_{u,d,s} \rightarrow PP$ decays, *Phys. Rev. D* **78**, 076002 (2008); K. Wang and G. Zhu, Flavor dependence of annihilation parameters in QCD factorization, *Phys. Rev. D* **88**, 014043 (2013); J. J. Wang, D. T. Lin, W. Sun, Z. J. Ji, S. Cheng, and Z. J. Xiao, $\bar{B}_s^0 \rightarrow K\pi$, KK decays and effects of the next-to-leading order contribution, *Phys. Rev. D* **89**, 074046 (2014); Q. Chang, J. Sun, Y. Yang, and X. Li, A combined fit on the annihilation corrections in $B_{u,d,s} \rightarrow PP$

- decays within QCDF, *Phys. Lett. B* **740**, 56 (2015); H. Y. Cheng, C. W. Chiang, and A. L. Kuo, Updating $B \rightarrow PP, VP$ decays in the framework of flavor symmetry, *Phys. Rev. D* **91**, 014011 (2015).
- [4] Q. Chang, X. Q. Li, and Y. D. Yang, A comprehensive analysis of hadronic $b \rightarrow s$ transitions in a family non-universal Z' model, *J. Phys. G* **41**, 105002 (2014).
- [5] S. Baek, D. London, J. Matias, and J. Virto, $B_s^0 \rightarrow K^+K^-$ and $B_s^0 \rightarrow K^0\bar{K}^0$ decays within supersymmetry, *J. High Energy Phys.* **12** (2006) 019; A. Hayakawa, Y. Shimizu, M. Tanimoto, and K. Yamamoto, Searching for the squark flavor mixing in CP violations of $B_s \rightarrow K^+K^-$ and $K^0\bar{K}^0$ decays, *Prog. Theor. Exp. Phys.* **2014**, 023B04 (2014).
- [6] C.-C. Peng *et al.* (Belle Collaboration), Search for $B_s^0 \rightarrow hh$ decays at the $\Upsilon(5S)$ resonance, *Phys. Rev. D* **82**, 072007 (2010).
- [7] C. Oswald *et al.* (Belle Collaboration), Semi-inclusive studies of semileptonic B_s decays at Belle, *Phys. Rev. D* **92**, 072013 (2015).
- [8] S. Esen *et al.* (Belle Collaboration), Precise measurement of the branching fractions for $B_s \rightarrow D_s^{(*)+}D_s^{(*)-}$ and first measurement of the $D_s^{*+}D_s^{*-}$ polarization using e^+e^- collisions, *Phys. Rev. D* **87**, 031101(R) (2013).
- [9] A. Abashian *et al.* (Belle Collaboration), The Belle detector, *Nucl. Instrum. Methods Phys. Res., Sect. A* **479**, 117 (2002); also see the detector section in J. Brodzicka *et al.*, Physics achievements from the Belle experiment, *Prog. Theor. Exp. Phys.* **2012**, 04D001 (2012).
- [10] Z. Natkaniec *et al.* (Belle SVD2 Group), Status of the Belle silicon vertex detector, *Nucl. Instrum. Methods Phys. Res., Sect. A* **560**, 1 (2006).
- [11] M. Feindt and U. Kerzel, The NEUROBAYES neural network package, *Nucl. Instrum. Methods Phys. Res., Sect. A* **559**, 190 (2006).
- [12] S. Brandt, C. Peyrou, R. Sosnowski, and A. Wroblewski, The principal axis of jets. An attempt to analyze high-energy collisions as two-body processes, *Phys. Lett.* **12**, 57 (1964).
- [13] G. C. Fox and S. Wolfram, Observables for the Analysis of Event Shapes in e^+e^- Annihilation and Other Processes, *Phys. Rev. Lett.* **41**, 1581 (1978); the modified moments used in this Letter are described in S. H. Lee *et al.* (Belle Collaboration), Evidence for $B^0 \rightarrow \pi^0\pi^0$, *Phys. Rev. Lett.* **91**, 261801 (2003).
- [14] D. J. Lange, The EVTGEN particle decay simulation package, *Nucl. Instrum. Methods Phys. Res., Sect. A* **462**, 152 (2001).
- [15] R. Brun *et al.*, GEANT 3.21, CERN Report No. DD/EE/84-1, 1984.
- [16] H. Albrecht *et al.* (ARGUS Collaboration), Search for hadronic $b \rightarrow u$ decays, *Phys. Lett. B* **241**, 278 (1990).
- [17] M. Pivk and F. R. Le Diberder, sPlot: A statistical tool to unfold data distributions, *Nucl. Instrum. Methods Phys. Res., Sect. A* **555**, 356 (2005).
- [18] R. Aaij *et al.* (LHCb Collaboration), Study of $B_{(s)}^0 \rightarrow K_S^0 h^+ h^-$ decays with first observation of $B_s^0 \rightarrow K_S^0 K^\pm \pi^\mp$ and $B_s^0 \rightarrow K_S^0 \pi^+ \pi^-$, *J. High Energy Phys.* **10** (2013) 143.
- [19] T. Abe *et al.* (Belle II Collaboration), Belle II Technical Design Report, arXiv:1011.0352.